International Journal of Thermophysics, Vol. 22, No. 1, 2001

Simulating Retention in Gas–Liquid Chromatography: Benzene, Toluene, and Xylene Solutes[1]

C. D. Wick,[2] M. G. Martin,[2,3] J. I. Siepmann,[2,4] and M. R. Schure[5]

Accurate predictions of retention times, retention indices, and partition constants are a long sought-after goal for theoretical studies in chromatography. Although advances in computational chemistry have improved our understanding of molecular interactions, little attention has been focused on chromatography, let alone calculations of retention properties. Configurational-bias Monte Carlo simulations in the isobaric–isothermal Gibbs ensemble were used to investigate the partitioning of benzene, toluene, and the three xylene isomers between a squalane liquid phase and a helium vapor phase. The united-atom representation of the TraPPE (transferable potentials for phase equilibria) force field was used for all solutes and squalane. The Gibbs free energies of transfer and Kovats retention indices of the solutes were calculated directly from the partition constants (which were averaged over several independent simulations). While the calculated Kovats indices of benzene and toluene at $T = 403$ K are significantly higher than their experimental counterparts, much better agreement is found for the xylene isomers at $T = 365$ K.

KEY WORDS: alkylbenzene; gas–liquid chromatography; molecular simulation; vapor–liquid equilibria.

1. INTRODUCTION

The underlying principles of chromatographic separation are inherently complex, being dictated by the interplay of the sample with the stationary

[1] Paper presented at the Fourteenth Symposium on Thermophysical Properties, June 25–30, 2000, Boulder, Colorado, U.S.A.

[2] Departments of Chemistry and of Chemical Engineering and Materials Science, 207 Pleasant Street SE, University of Minnesota, Minneapolis, Minnesota 55455-0431, U.S.A.

[3] Present address: Computational Biology and Materials Technology, Sandia National Laboratories, P.O. Box 5800, Albuquerque, New Mexico 87185-1111, U.S.A.

[4] To whom correspondence should be addressed.

[5] Theoretical Separation Science Laboratory, Rohm and Haas Company, 727 Norristown Road, Spring House, Pennsylvania 19477, U.S.A.

0195-928X/01/0100-0111$19.50/0

phase (solid substrate and bonded phase) and the mobile phase, which often contains a mixture of solvents. Thus, predicting the retention characteristics of a solute molecule given only its structure (types of atoms and their connectivity) and the experimental chromatographic conditions (temperature, pressure, stationary and mobile phase compositions) remains one of the grand challenges in separation science. Many methods for the prediction of retention data have appeared in the literature [1–5].

Of all of the various chromatographic techniques, gas–liquid chromatography (GLC or just GC) is perhaps the simplest system to study on a fundamental level. This is due to the rather well-defined nature of a gas in equilibrium with a high boiling temperature liquid typically coated on the inner surface of a fused silica capillary. We have previously demonstrated that configurational-bias Monte Carlo simulations in the Gibbs ensemble using transferable force fields can be carried out to successfully predict the retention order of alkane isomers in helium–squalane (2,6,10,15,19,23-hexamethyltetracosane) GLC and to provide insights into the thermodynamic driving forces of the chromatographic retention processes [6].

The aim of this research is to extend our previous calculations on retention in helium–squalane GLC to aromatic solutes, such as benzene, toluene, the xylene isomers, and, at a later point, also naphthalene and larger polycyclic aromatic hydrocarbons. Squalane is a widely used liquid phase in GLC [7] and the reference material for the Rohrschneider–McReynolds scheme of liquid phase characterization [8, 9]. The remainder of this article is divided as follows. The next section is devoted to a brief description of the force fields used for alkanes and aromatics and of the simulation methodology. Thereafter, the results for the partitioning of aromatics are discussed.

2. FORCE FIELDS AND SIMULATION DETAILS

For the past 5 years, our group has employed calculations of vapor–liquid coexistence curves (VLCC) of model compounts and their mixtures to develop the TraPPE (transferable potentials for phase equilibria) force fields [10–14]. The TraPPE-UA (united-atom) force field for hydrocarbons, in which entire methyl, methylene, and methine units (see Table I) are treated as *pseudo*-atoms, is based on a relatively simple functional form to calculate the potential energy of the system. The nonbonded interactions between *pseudo*-atoms, which are separated by more than three bonds or belong to different molecules, are described by pairwise-additive Lennard–Jones (LJ) 12–6 potentials

$$u(r_{ij}) = 4\varepsilon_{ij}\left[\left(\frac{\sigma_{ij}}{r_{ij}}\right)^{12} - \left(\frac{\sigma_{ij}}{r_{ij}}\right)^{6}\right] \tag{1}$$

Table I. Summary of Lennard–Jones Parameters Used in the TraPPE-UA Force Field

Pseudo-atom	σ (Å)	ε/k_B (K)
Helium	3.11	4.0
CH_3 (sp3)	3.75	98.0
CH_2 (sp3)	3.95	46.0
CH (sp3)	4.65	10.0
CH (aro)	3.695	50.5
R–C (aro)	3.88	21.0

where r_{ij}, ε_{ij}, and σ_{ij} are the separation, LJ well depth, and LJ size, respectively, for the pair of atoms i and j. Calculated VLCC and other phase equilibria are extremely sensitive to very small changes of the nonbonded force field parameters. Thus, the LJ parameters for the TraPPE force field were determined from single-component VLCC [10–14]. The values of these parameters are listed in Table I. The parameters for unlike interactions are computed using standard Lorentz–Berthelot combining rules [15]. Spherical potential truncations at 14 Å and analytical tail corrections (for the energy, pressure, and chemical potential) were used for the Lennard–Jones interactions [15].

As in other common molecular mechanics force fields [16, 17], the TraPPE-UA force field uses a set of bonded potentials to describe the intramolecular interactions for *pseudo*-atoms that are separated by three or less bonds. The bond lengths are fixed using values of 1.54 and 1.40 Å for carbon–carbon single bonds and for aromatic rings, respectively. In addition, benzene, toluene, and the xylenes are modeled as rigid, planar structures [14], whereas harmonic bond angle bending potentials and cosine series dihedral potentials are used for linear and branched alkanes [11]. The parameters for these intramolecular interactions of squalane can be found in Ref. 11.

The position of chemical and phase equilibria as well as the retention of solutes in chromatographic systems is determined by free energies. The partition constant of solute S between phase α and phase β is directly related to the Gibbs free energy of transfer [18]

$$\Delta G_S = RT \ln\left(\frac{\rho_S^\alpha}{\rho_S^\beta}\right) \tag{2}$$

where ρ_S^α and ρ_S^β are the number densities of S in the two phases at equilibrium, and the ratio of these is the partition constant K. The partition

constant, K, and the retention time, t_r, of a solute are related as follows [19]:

$$\phi K = \frac{t_r}{t_0} - 1 \tag{3}$$

where ϕ and t_0 are the phase ratio and the void time (elution time of an unretained compound), respectively. At $T = 365$ K (used in some of the GLC simulations described below), a dramatic change in the partition constant (or relative retention time), say by a factor 2, is associated with a relatively small change in free energy of $\Delta G^\circ = 2.1\ \text{kJ} \cdot \text{mol}^{-1}$ [20]. A 10% change in the partition constant requires only $0.29\ \text{kJ} \cdot \text{mol}^{-1}$. Whereas the determination of mechanical properties is now routine for computer simulation, the determination of (relative and absolute) free energies and other thermal properties, which depend on the volume of phase space, remains one of the most challenging problems [15, 21].

Over the past few years many new methods have been proposed which greatly aid in the calculation of phase equilibria [21–27]. The simulations described herein were carried out using a combination of the Gibbs-ensemble Monte Carlo (GEMC) method [28–30] and the configurational-bias Monte Carlo (CBMC) algorithm [11, 31–34]. GEMC utilizes two separate simulation boxes that are in thermodynamic contact but do not have an explicit interface (see Fig. 1). Simulations for single-component systems are conveniently carried out in the canonical version of the Gibbs ensemble where the combined volume of the two simulation boxes remains fixed and mechanical equilibrium is reached by volume exchanges between the two

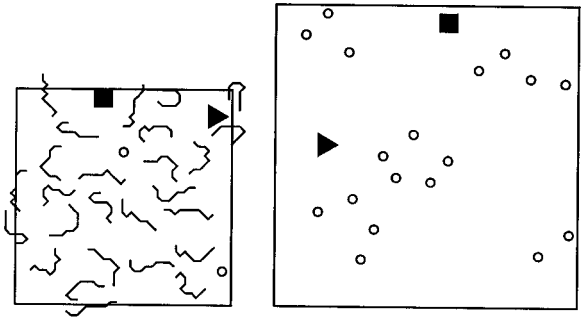

Fig. 1. Schematic drawing of the Gibbs ensemble setup used to study the partitioning of two solutes (filled squares and triangles) between a squalane liquid phase (chains) and a helium vapor phase (small open circles).

boxes. For multicomponent systems the isobaric–isothermal version of the Gibbs ensemble is more appropriate where volume exchanges with an external pressure bath are performed to reach mechanical equilibrium with a prespecified external pressure. Another of the GEMC moves involves the swapping of a molecule from one phase to the other, thereby equalizing the chemical potentials of each species in the two phases. Acceptance of these particle interchanges is often the rate-limiting step in GEMC simulations, and to improve the sampling of insertions of flexible molecules, such as the alkanes, the CBMC technique is used. CBMC replaces the conventional random insertion of entire molecules with a scheme in which the chain molecule is inserted atom by atom such that conformations with favorable energies are preferentially found. The resulting bias in the CBMC swap step, which improves the efficiency of the simulations by many orders of magnitude, is then removed by using special acceptance rules [35, 36]. In addition to volume and swap moves, one needs to carry out translational, rotational, and conformational moves on randomly selected molecules to reach thermal equilibrium.

For a given state point the properties of the coexisting phases can be determined directly from a single GEMC simulation. Since a GEMC simulation samples the partitioning of solutes (and also solvents) between two phases, it can also be used to calculate the partition constant directly from the ratio of the number densities or, if so desired, also using the molality scale. Knowing the partition constant, K, the free energy of transfer, ΔG°, can be calculated directly from Eq. (2), which is the same procedure as used for experimental data. Similar to experimental procedures, the partitioning of multiple solutes can be obtained from one simulation [37–39]. The precision of our calculations can also be enhanced by adjusting the phase ratio to yield roughly equal relative errors in the number densities in both phases [37].

In the special case of simulations for GLC systems, particle swap moves have to be performed only for the solutes and the carrier gas. Since the liquid phase in GLC is used only over a temperature range where its vapor pressure is negligible, there is no need to sample the partitioning of squalane. Two groups of 10 independent simulations were carried out, where each group sampled the partitioning of five solutes: (i) system BEN/TOL—*n*-hexane, *n*-heptane, *n*-octane, benzene, and toluene; and (ii) system XYL—*n*-octane, *n*-nonane, and *o*-, *m*-, and *p*-xylene. The simulation systems consisted of 96 squalane molecules, a total of 10 solute (2 each) molecules, and 500 helium atoms. The external pressure was set to 101.5 kPa for both systems, but different temperatures were used: 403 K for system BEN/TOL and 365 K for system XYL. The total lengths of the production periods were 4.5 and 5.5×10^5 Monte Carlo cycles for the BEN/TOL and XYL

systems, respectively (one Monte Carlo cycle consists of N attempted moves, with N being the total number of molecules).

3. RESULTS AND DISCUSSION

The single-component VLCCs for benzene, toluene, and the three xylene isomers are shown in Figs. 2 and 3. The TraPPE-UA LJ parameters for the aromatic groups (see Table I) were determined from calculations of the vapor–liquid equilibria of benzene for CH(aro) and toluene for R–C(aro) [14]. The VLCCs of benzene and toluene are well reproduced by the TraPPE-UA force field. As was also found for the alkanes and alkenes [10, 11, 14], agreement with experimental saturated liquid densities [40] is very good (less than 1% deviation over the entire temperature ranges), but vapor pressures and densities are slightly overpredicted. Although the normal boiling points are underestimated by about 3%, the critical temperatures are very close to their experimental counterparts [40].

Once the force field parameters for CH(aro) and R–C(aro) are set from the benzene and toluene simulations (and for the methyl group from

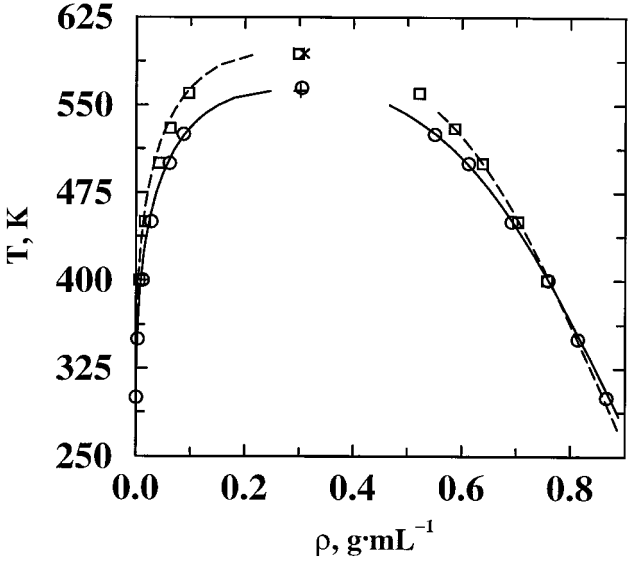

Fig. 2. Vapor–liquid coexistence curves for benzene and toluene. Calculated coexistence densities and extrapolated critical points for the TraPPE-UA force field [14] are depicted as circles and squares, respectively. Experimental coexistence curves [40] and critical points are shown as follows: benzene, solid lines and +; toluene, dashed lines and ×.

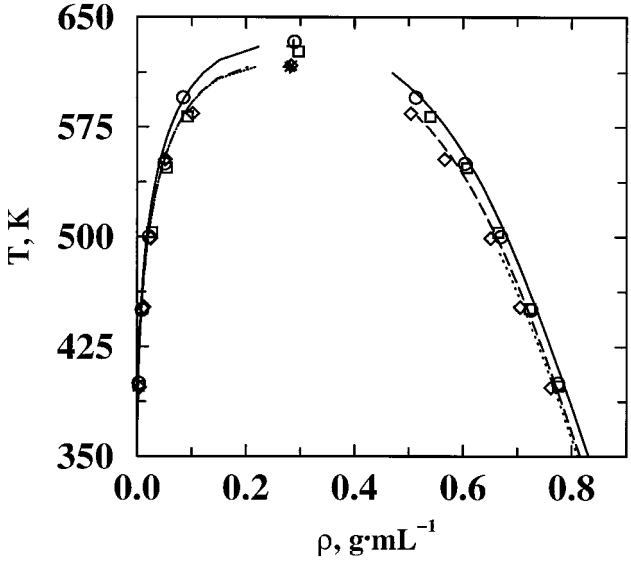

Fig. 3. Vapor–liquid coexistence curves for *o*-, *m*-, and *p*-xylene. Calculated coexistence densities and extrapolated critical points for the TraPPE-UA force field [14] are depicted as circles, squares, and diamonds, respectively. Experimental coexistence curves [40] and critical points are shown as follows: *o*-xylene, solid lines and +; *m*-xylene, long-dashed lines and ×; and *p*-xylene, dotted lines and ∗.

simulations of ethane), there remain no adjustable parameters for simulations of the xylene isomers. Considering the relative simplicity of the TrAPPE-UA force field, the VLCCs of the three xylene isomers are remarkedly well reproduced. The calculated orthobaric liquid densities deviate by about 2% from experimental data [40], with the largest deviations observed for *m*-xylene at higher temperatures. However, the relative ordering of the VLCCs is not predicted with quantitative accuracy. Whereas the experimental liquid densities, critical temperatures, and normal boiling points of *m*- and *p*-xylene are close, the TraPPE-UA force field predicts smaller differences between *o*- and *m*-xylene. In contrast, the relative differences between *o*- and *p*-xylene are in good agreement with experiment [40].

The calculated partition constants and Gibbs free energies of transfer, ΔG, for helium and the alkane and alkyl benzene solutes are listed in Table II. For all solutes, the statistical errors in ΔG are smaller than $0.2\ \mathrm{kJ \cdot mol^{-1}}$, which is sufficient to separate solutes whose retention times differ by less than 10%. As expected, the differences in the free energies of

Table II. Summary of Simulation Results: Partition Constants, Gibbs Free Energies of Transfer, and Kovats Retention Indices[a]

Molecule	T (K)	K	ΔG (kJ · mol^{-1})	I_{sim}	I_{exp}
Helium	403	0.0626_3	$+9.28_4$		
n-Hexane	403	17.0_4	-9.50_8	600	600
Benzene	403	30.6_5	-11.47_5	694_9	656
n-Heptane	403	32.3_{11}	-11.65_{11}	700	700
Toluene	403	56.5_{10}	-13.40_6	794_{11}	764
n-Octane	403	60.6_{19}	-13.75_{11}	800	800
Helium	365	0.0466_3	$+9.30_6$		
n-Octane	365	170_6	-15.60_{11}	800	800
o-Xylene	365	331_{10}	-17.62_9	890_9	883
m-Xylene	365	262_7	-16.90_8	858_7	863
p-Xylene	365	285_9	-17.16_9	870_8	861
n-Nonane	365	356_{13}	-17.84_{12}	900	900

[a] The subscripts give the statistical uncertainties in the last digit(s). The experimental data were taken from Refs. 44 and 45.

transfer between the xylene isomers are relatively small. Comparison of the partitioning of *n*-octane at 365 K (system XYL) and at 403 K (system BEN/TOL) shows the expected decrease in the magnitude of ΔG with increasing temperature. The Martin equation predicts that the Gibbs free energies of transfer (and also the net retention times) are a linear function of the number of carbon atoms, n, in any homologous series

$$\Delta G_n^* = A + B \times n \tag{4}$$

Three *n*-alkanes were present in system BEN/TOL ($T = 403$ K), and their calculated ΔG's of the *n*-alkanes indicate linearity, at least, within the accuracy of the simulations and yield a methylene group increment of about 2.1 kJ · mol^{-1}. The difference of approximately 2.2 kJ · mol^{-1} in ΔG for *n*-octane and *n*-nonane in system XYL ($T = 365$ K) is slightly larger. These values are consistent with the previously calculated methylene increment of 2.39 ± 0.10 kJ · mol^{-1} from *n*-pentane to *n*-octane at $T = 343$ K [6].

Absolute Gibbs free energies of transfer are rarely measured for most chromatographic experiments because the ratio of the mobile to stationary phase volumes must be known for the calculation of equilibrium constants [see Eq. (3)]. This phase ratio differs from column to column and often is difficult to measure accurately. Thus, it has proven more useful to use the concept of a retention index to give the relative retention time of a given

solute [41]. The Kovats retention index I of a solute x can be calculated directly from the partitioning using [42, 43]

$$I_x = 100n + 100\left[\frac{\log(K_x/K_n)}{\log(K_{n+1}/K_n)}\right] \tag{2}$$

where K_x, K_n, and K_{n+1} are the partition constants of the solute in question, the highest normal alkane (having n carbon atoms) that elutes prior to the solute, and the lowest normal alkane (having $n+1$ carbon atoms) that elutes after the solute, respectively. That is, the Kovats index of an n-alkane is $100n$, and an index of, say, 650 means that this solute would elute together with a fictitious normal alkane having 6.50 carbon atoms.

The calculated Kovats retention indices are compared to their experimental counterparts in Fig. 4, and the numerical values are listed in Table II. It is very encouraging that the elution order of the n-alkanes and the alkylbenzene are rather well reproduced and that I values can be predicted with a statistical precision (error of the mean) of about 10

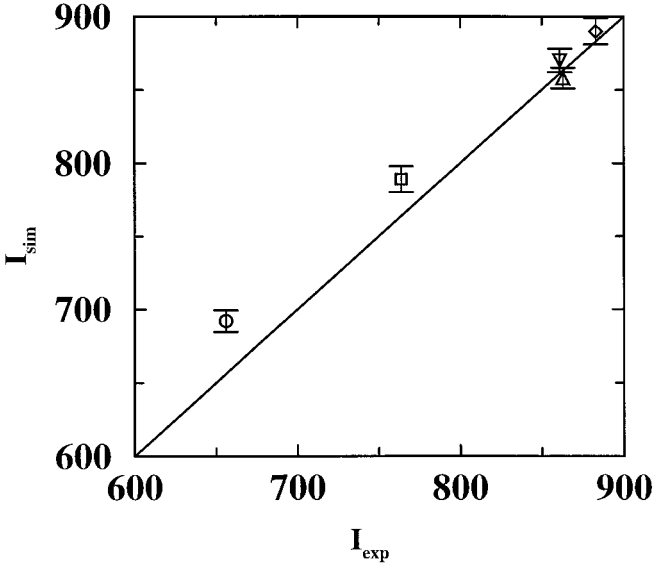

Fig. 4. Predicted Kovats retention indices of benzene (circle; $T = 403$ K), toluene (square; $T = 403$ K), *o*-, *m*-, and *p*-xylene (diamond, up triangle and down triangle, respectively; $T = 365$ K) for a helium–squalane gas–liquid chromatography system. The experimental data were taken from Refs. 44 and 45.

Kovats units. Whereas the I values for the three xylene isomers are in in satisfactory agreement with experiment [44] (root mean square error of about 7 Kovats units), the calculated I values for benzene and toluene are markedly higher than experiment [45]. Currently we can only speculate on the causes for these large deviations in the I values for benzene and toluene. The most likely candidate might be the neglect of quadrupolar interactions in our alkylbenzene force field which would have the most pronounced effect for benzene and decreasing importance with the number of methyl group substituents. Another cause could be the relatively high temperature of 403 K at which the experiments and simulations were carried out. Clearly additional simulation studies are required to explore whether lowering the temperature or including quadrupolar interactions will lead to better agreement. Finally, it should be noted that although the predicted I values for *o*- and *p*-xylene show (small) positive deviations from experiment, the I value for *m*-xylene is underestimated. Here we would like to argue that this is related to shortcomings in the force field that were already noted for the single-component VLCC (see above).

4. CONCLUSIONS

The rapid development of more efficient simulation algorithms, more accurate force fields, and more powerful computers is now permitting the use of molecular simulations for the investigation of complex problems in thermodynamics that were hitherto intractable. The combination of Gibbs-ensemble Monte Carlo and configurational-bias Monte Carlo allows the efficient and precise determination of single- and multicomponent phase diagrams and of partition constants. In conjunction with the TraPPE-UA force field, we were able to predict satisfactorily the retention order of alkanes and alkylbenzenes in helium–squalane gas–liquid chromatography. Nevertheless, further improvements in force fields are clearly desirable to improve the quantitative accuracy of the predicted retention indices. The authors hope that molecular simulations of chromatographic systems will become an essential tool for providing a molecular-level understanding of the factors contributing to the retention process and for predicting retention times.

ACKNOWLEDGMENTS

We thank Pete Carr and Ray Mountain for many stimulating discussions. Financial support from the National Science Foundation (CHE-9816328), a Sloan Research Fellowship, and Department of Energy Computational Science Graduate Fellowships (C.D.W. and M.G.M.) is gratefully

acknowledged. A very generous amount of computer time was provided by the Minnesota Supercomputing Institute.

REFERENCES

1. B. L. Karger, L. R. Snyder, and C. Eon, *Anal. Chem.* **50**:2126 (1978).
2. W. R. Melander and C. Horváth, in *High-Performance Liquid Chromatography: Advances and Perspectives*, *Vol. 2*, C. Horváth, ed. (Academic Press, London, 1980), p. 113.
3. D. E. Martire and R. E. Boehm, *J. Phys. Chem.* **87**:1045 (1983).
4. R. Kaliszan, *Quantitative Structure–Chromatographic Retention Relationships*, Chemical Analysis, Vol. 93 (Wiley-Interscience, New York, 1987).
5. C. H. Lochmüller, C. Reese, A. J. Aschman, and S. J. Breiner, *J. Chromatogr. A* **656**:3 (1993).
6. M. G. Martin, J. I. Siepmann, and M. R. Schure, *J. Phys. Chem. B* **103**:11191 (1999).
7. D. A. Tourres, *J. Chromatogr.* **30**:357 (1967).
8. L. Rohrschneider, *J. Chromatogr.* **22**:6 (1966).
9. W. O. McReynolds, *J. Chromatogr. Sci.* **8**:685 (1970).
10. M. G. Martin and J. I. Siepmann, *J. Phys. Chem. B* **102**:2569 (1988).
11. M. G. Martin and J. I. Siepmann, *J. Phys. Chem. B* **103**:4508 (1999).
12. B. Chen and J. I. Siepmann, *J. Phys. Chem. B* **103**:5370 (1999).
13. B. Chen, J. Xing, and J. I. Siepmann, *J. Phys. Chem. B* **104**:2391 (2000).
14. C. D. Wick, M. G. Martin, and J. I. Siepmann, *J. Phys. Chem. B* **104**:8008 (2000).
15. M. P. Allen and D. J. Tildesley, *Computer Simulation of Liquids* (Oxford University Press, Oxford, 1987).
16. W. D. Cornell, P. Cieplak, C. Bayly, I. R. Gould, K. M. Merz, D. M. Ferguson, D. C. Spellmeyer, T. Fox, J. W. Caldwell, and P. A. Kollman, *J. Am. Chem. Soc.* **117**:5179 (1995).
17. W. L. Jorgensen, D. S. Maxwell, and J. Tirado-Rives, *J. Am. Chem. Soc.* **118**:11225 (1996).
18. A. Ben-Naim, *Statistical Thermodynamics for Chemists and Biochemists* (Plenum Press, New York, 1992).
19. J. C. Giddings, *Unified Separation Science* (Wiley, New York, 1991).
20. M. R. Schure, in *Advances in Chromatography*, *Vol. 39*, P. R. Brown and E. Grushka, eds. (Marcel Dekker, New York, 1998), p. 139.
21. D. Frenkel and B. Smit, *Understanding Molecular Simulation* (Academic Press, New York, 1996).
22. J. P. Valleau, *J. Chem. Phys.* **99**:4718 (1993).
23. S. K. Kumar, I. Szleifer, and A. Z. Panagiotopoulos, *Phys. Rev. Lett.* **66**:2935 (1991).
24. D. A. Kofke, *J. Chem. Phys.* **98**:4149 (1993).
25. N. B. Wilding, *Phys. Rev. E* **52**:602 (1995).
26. F. A. Escobedo and J. J. de Pablo, *J. Chem. Phys.* **106**:2911 (1997).
27. T. Spyriouni, I. G. Economou, and D. N. Theodorou, *Phys. Rev. Lett.* **80**:4466 (1998).
28. A. Z. Panagiotopoulos, *Mol. Phys.* **61**:813 (1987).
29. A. Z. Panagiotopoulos, N. Quirke, M. Stapleton, and D. J. Tildesley, *Mol. Phys.* **63**:527 (1988).
30. B. Smit, P. de Smedt, and D. Frenkel, *Mol. Phys.* **68**:931 (1989).
31. J. I. Siepmann, *Mol. Phys.* **70**:1145 (1990).
32. J. I. Siepmann and D. Frenkel, *Mol. Phys.* **75**:59 (1992).
33. D. Frenkel, G. C. A. M. Mooij, and B. Smit, *J. Phys. Cond. Matt.* **4**:3053 (1992).

34. J. J. de Pablo, M. Laso, and U. W. Suter, *J. Chem. Phys.* **96**:2395 (1992).
35. G. C. A. M. Mooij, D. Frenkel, and B. Smit, *J. Phys. Cond. Matt.* **4**:L255 (1992).
36. M. Laso, J. J. Pablo, and U. W. Suter, *J. Chem. Phys.* **97**:2817 (1992).
37. M. G. Martin and J. I. Siepmann, *J. Am. Chem. Soc.* **119**:8921 (1997).
38. M. G. Martin and J. I. Siepmann, *Theor. Chem. Acc.* **99**:347 (1998).
39. B. Chen and J. I. Siepmann, *J. Am. Chem. Soc.* **122**:6464 (2000).
40. B. D. Smith and R. Srivastava, *Thermodynamic Data for Pure Compounds: Part A. Hydrocarbons and Ketones* (Elsevier, Amsterdam, 1986).
41. M. V. Budahegyi, E. R. Lombosi, T. S. Lombosi, S. Y. Mészáros, Sz. Nyiredy, G. Tarján, I. Timár, and J. M. Takács, *J. Chromatogr.* **271**:213 (1983).
42. E. Kovats, *Helv. Chim. Acta* **41**:1915 (1958).
43. E. Kovats, in *Advances in Chromatography*, *Vol. 1* (Marcel Dekker, New York, 1965), p. 229.
44. J. Krupcik, O. Liska, and L. Sojak, *J. Chromatogr.* **51**:119 (1970).
45. L. E. Cook and F. M. Raushel, *J. Chromatogr.* **65**:556 (1972).